Rivista Italiana di Paleontologia e Stratigrafia
(*Research in Paleontology and Stratigraphy*)
vol. 129(1): 91-110. **March 2023**
DOI: https://doi.org/10.54103/2039-4942/17769

THE DISTRIBUTION RANGE OF CALCAREOUS NANNOFOSSIL SPECIES *RETICULOFENESTRA PSEUDOUMBILICUS* IN THE MIOCENE: AN EXAMPLE OF ECOLOGICAL INFLUENCE ON EVOLUTIONARY DEVELOPMENT.

AMALIA NOTARO*[1], ISABELLA RAFFI[1] & DANIELE REGHELLIN[2]

[1]Dipartimento di Ingegneria e Geologia, Università degli Studi "G. d'Annunzio" di Chieti-Pescara, I-66013 Chieti Scalo, Italy.
E-mail: amalia.notaro@unich.it
[2]Dipartimento di Scienze Pure e Applicate (DiSPeA), Università degli Studi di Urbino "Carlo Bo", Urbino, Italy.
*Corresponding Author.

Associate Editor: Silvia Gardin.

To cite this article: Notaro A., Raffi I. & Reghellin D. (2023) - The distribution range of calcareous nannofossil species *Reticulofenestra pseudoumbilicus* in the Miocene: an example of ecological influence on evolutionary development. *Riv. It. Paleontol. Strat.*, 129(1): 91-110.

Keywords: calcareous nannofossils; *Reticulofenestra*; Neogene; morphometry.

Abstract. Reticulofenestra pseudoumbilicus is a Neogene calcareous nannofossil species whose highest stratigraphic occurrence (Top) is a reliable biohorizon in the Pliocene, calibrated at 3.82 Ma. The species is present in the stratigraphic record from at least the Middle Miocene, within an interval around the biohorizon Top *Sphenolithus heteromorphus*, calibrated at 13.53 Ma, but its lower distribution range is not precisely delineated. The study of nannofossil assemblages in sediment cores from Integrated Ocean Drilling Program IODP Site U1338 (eastern equatorial Pacific) indicates a lower stratigraphic position for the evolutionary emergence (Base) of *R. pseudoumbilicus,* detected in the Early Miocene with an estimated age of 16.46 Ma. This age results from a new astronomically tuned chronology, which dates the deepest sediments at Site U1338 to 16.67 Ma. Base *R. pseudoumbilicus* is followed above by a temporary disappearance of the taxon until a re-entrance after ~3 Myr. This lengthened stratigraphic range has been confirmed by data from other locations at low and mid-latitudes in the Atlantic. The distribution range of *R. pseudoumbilicus*, lasting ~13 Myr during the Neogene, is thus characterized by a variable pattern of repeated occurrences and disappearances. Comparison to benthic foraminifera $\delta^{18}O$ and $\delta^{13}C$ records suggests a control by global climatic/environmental conditions on these events, particularly by temperature variations. The recurrent presence of *R. pseudoumbilicus* at stratigraphically different intervals could represent an example of iterative evolution, expressed as repeated speciation events that are in part influenced by complex external factors related to the dynamic climate and environmental evolution during the Miocene.

Introduction

The species *Reticulofenestra pseudoumbilicus* (Gartner, 1969) is a well-known Neogene taxon and a characteristic component of calcareous nannofossil assemblages in the Miocene to Pliocene stratigraphic interval. The genus *Reticulofenestra* is the basic taxon of the Noëlaerhabdaceae family, dominant in the nannofossil/nannoplankton assemblages since the early Eocene. The last occurrence (Top) of *R. pseudoumbilicus* is a reliable biostratigraphic biohorizon, astronomically calibrated at 3.82 Ma (Backman et al. 2012) and used in the mid-Pliocene to recognize the equivalent zonal boundaries NN15/NN16 (in Martini's 1971 zonation), CN11b/CN12a (in Okada and Bukry's 1980 zonation), and CNPL3/CNPL4 (in Backman et al.'s 2012 zonation). Specimens with a wide range of size were included in the

Received: April 29, 2022; accepted: January 18, 2023

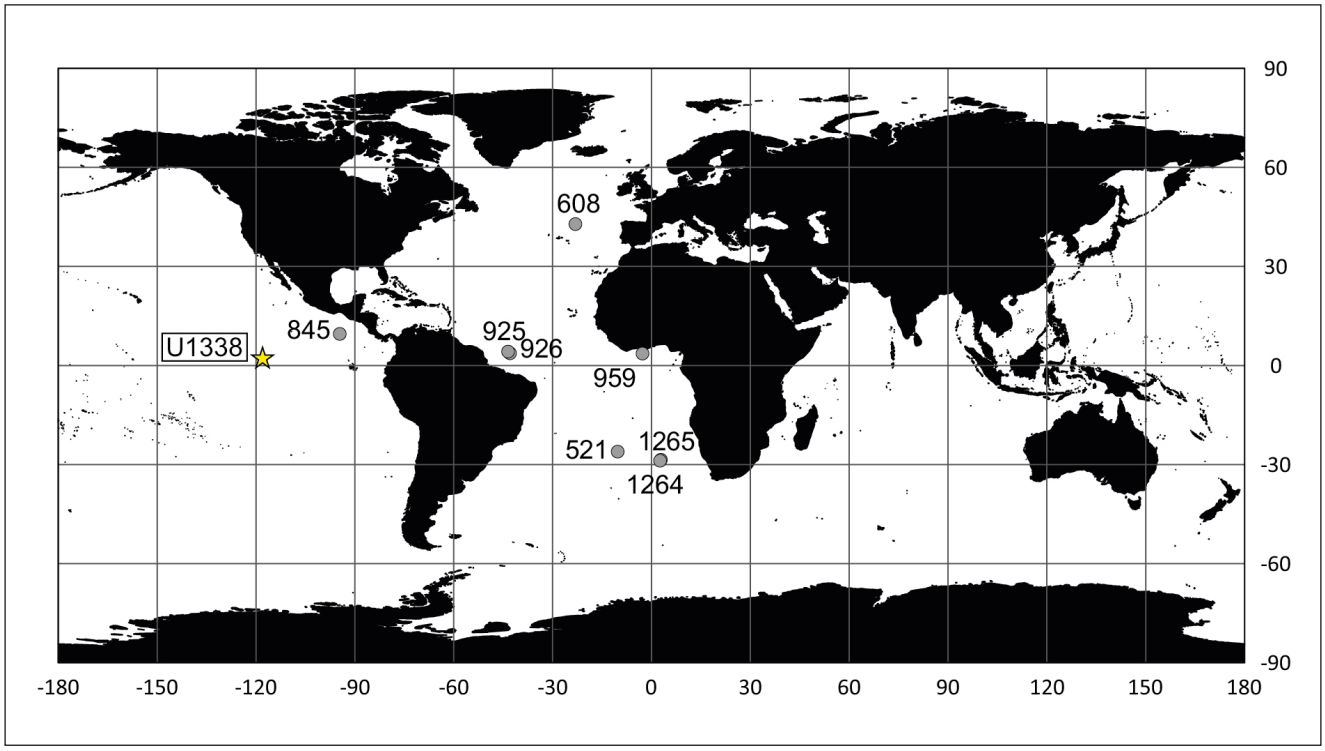

Fig. 1 - Location map with the sites considered in the present study. U1338, 845 (Pacific Ocean), 608, 925, 959, 521, 1264, 1265 (Atlantic Ocean).

taxonomic definition of *R. pseudoumbilicus* (major axis ranging from 5 to 8 μm), resulting in different stratigraphic positions for its last occurrence biohorizon. Several authors suggested to distinguish larger (major axis > 7 μm) specimens from smaller (< 7 μm) specimens for biostratigraphic purpose (Raffi & Rio 1979; Backman & Shackleton 1983; Rio et al. 1990a, b; Young 1990). In fact, in the Pliocene only the larger specimens provide an unambiguously recognized biohorizon (defined as "Top of *R. pseudoumbilicus*" in Backman et al. 2012), useful for biostratigraphy. The complete stratigraphic range of this taxon has been vaguely delineated in its lower part due to an unclear position of the lowermost occurrence in the Lower to Middle Miocene interval. In a preliminary biostratigraphic analysis of nannofossil assemblages in Lower-Middle Miocene sediment cores of IODP Site U1338, located in the Eastern Equatorial Pacific (EEP) (Pälike et al. 2010), occurrences of reticulofenestrids including the typical "larger" *R. pseudoumbilicus* were recorded (Fig. 1). The presence of these "large" forms and the availability of high-resolution samples in the sedimentary succession of IODP Site U1338, led us to investigate in detail on the lower distribution range of *R. pseudoumbilicus* to determine the appearance pattern of the taxon. We aimed to minimize uncertainty of the position of its lowermost occurrence biohorizon, comparing the results with data from different locations, and tried to draw an analogy with the abundance fluctuations of the taxon occurring in the Late Miocene. We compared the *R. pseudoumbilicus* abundance pattern to stacked benthic foraminifera $\delta^{18}O$ and $\delta^{13}C$ records (Westerhold et al. 2020), to highlight potential correlations between these fluctuations and variations of paleoclimatic/paleoenvironmental conditions.

Taxonomic remarks

In this study we focused on elliptical specimens of *R. pseudoumbilicus* having a major axis length of 7 to 11 μm, according to the taxonomic concept used for the Pliocene biohorizon Top (T) *R. pseudoumbilicus* that represents the exit of the taxon from the stratigraphic record. Although previous authors indicated a major axis size larger than 7 μm for this taxon to be biostratigraphically useful (e.g. Rio et al. 1990a; Raffi et al. 1995), specimens of 7 μm in size are included within our "large *R. pseudoumbilicus*" concept because they have the same pattern of

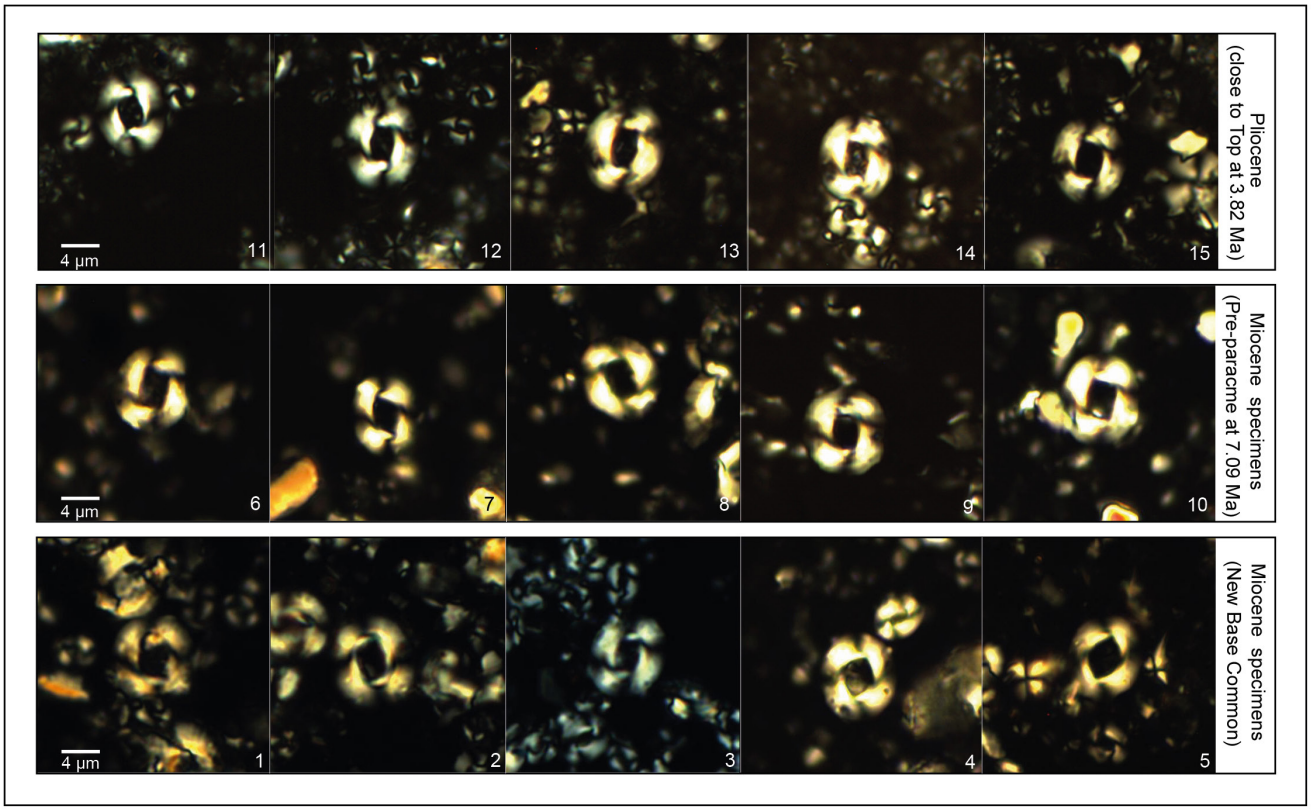

Fig. **2** - Comparison of *R. pseudoumbilicus* specimens from and lower Miocene interval (1-3: sample U1338C-46H-3,120 cm; 4-5: sample U1338B-42H-4,80 cm), upper Miocene interval (6-7: sample U1338C-37H-2,47 cm; 8-10: sample U1338B-36H-5,122 cm) and Pliocene interval (11-13: sample U1338B-6H-5,120 cm; 14-15: sample U1338B-5H-2,120 cm). Photomicrographs at X1200 magnification, cross-polarized light.

occurrence as the larger specimens (8 to 11 µm in size). This Neogene *Reticulofenestra* morphospecies is clearly distinct from medium size (major axis 5-6 µm in length) and smaller size (major axis ≤ 4 µm) reticulofenestrids that are taxonomically distinguished into the species *Reticulofenestra haqii*, *Reticulofenestra minutula*, and *Reticulofenestra minuta*.

A perfect resemblance of the large *R. pseudoumbilicus* specimens observed in the Lower-Middle Miocene sediments with specimens from the Upper Miocene and Pliocene sections results from direct comparison (Fig. 2).

The stratigraphic distribution of *Reticulofenestra pseudoumbilicus*

As in the Pliocene nannofossil assemblages, *R. pseudoumbilicus* is a common component in the Upper Miocene. Notably, within this interval a temporary disappearance of the taxon (called "Paracme" or "Absence interval") has been recorded as concomitantly occurring in different oceanic areas (Rio et al. 1990a; Young 1990; Gartner 1992; Takayama 1993; Raffi et al. 1995; Backman & Raffi 1997; Raffi et al. 2003). This "Absence interval" extended from 8.8 Ma to ~7.1 Ma (astronomically calibrated ages; Backman et al. 2012). Data are more unresolved for the lower part of the distribution range of *R. pseudoumbilicus* and the first occurrence (Base) biohorizon has not been precisely defined and calibrated. Previous studies in few sections from low to mid-latitudes reported a sporadic and discontinuous presence of large *R. pseudoumbilicus* specimens in the Lower Miocene (between ~18 and ~15 Ma) (Rio et al. 1990a; Raffi et al. 1995; Maiorano & Monechi 1998; Foresi et al. 2014), followed above by an increase in abundance of the taxon with a more continuous range. Specifically, this increase, defined as Base common *R. pseudoumbilicus* biohorizon, has been recorded close (just below or above) to the biohorizon T *Sphenolithus heteromorphus* (Rio et al. 1990a; Raffi et al. 1995) astronomically calibrated at 13.53 Ma (Backman et al. 2012). Different stratigraphic positions for this increase in abundance and, in general, differences in the lower distribution

pattern of *R. pseudoumbilicus* were observed at different locations (e.g. Olafsson 1991; Fornaciari et al. 1993; Raffi & Flores 1995; Raffi et al. 1995). The beginning of the continuous distribution range of *R. pseudoumbilicus* >7 μm in the Upper Miocene seemed to begin in an upper stratigraphic level (slightly later) at mid-latitudes than in tropical/equatorial regions (Fornaciari et al. 1993; Raffi et al. 1995). Note that this uncertainty in depicting the lower stratigraphic distribution of the taxon could be in part the result of the different taxonomic definition used, even if a paleoecological control cannot be entirely ruled out.

Material and methods

Data on the distribution range of *R. pseudoumbilicus* have been collected from IODP Site U1338 in detail and, for comparison, from other locations (Fig. 1) in which only partial distribution patterns have been obtained, mostly in low resolution sampling sets. IODP Site U1338, located at 2° 30.469' N, 117° 58.174' W at a water depth of 4210 m, was drilled during IODP Expedition 320/321, the so-called Pacific Equatorial Age Transect (PEAT; Pälike et. al 2010) comprising a series of sites on the paleoequator at key intervals in the evolution of the Cenozoic climate. Together with Site U1337, Site U1338 was targeted to study paleoclimatic and paleoceanographic evolution during the Neogene in this important oceanic area that is intricately linked to major changes in the global climate system that took place during the Cenozoic (Lyle et al. 2010). Several studies were carried out in the last decade on Exp. 320/321 sediments that represent reference records for studies on global climatic changes and carbon cycle variations during the Neogene (e.g., Holbourn et al. 2014, 2015; Kochhann et al. 2017; Drury et al. 2017; Westerhold et al. 2020). Here we studied the lower interval of the composite section of Site U1338 derived by the splicing together sections of Holes U1338B and U1338C revised by Wilkens et al. (2013). Depth data for the section have been obtained following Backman et al. (2016) and resulted in corrected composite depths (CCSF-B) in meters - m -, used throughout the text.

The 186 analysed samples span ~32 m of sediments, and have variable sampling resolution, ranging from high (1 sample/10 cm) to low resolution (1 sample/75 cm). Analyses of nannofossil assemblages were also carried out in selected stratigraphic intervals at Ocean Drilling Program (ODP) Sites 925 (25 samples analysed) and 959 (85 samples) from the western and eastern equatorial Atlantic respectively, Deep Sea Drilling Project (DSDP) Site 608 from the mid-latitude North Atlantic (79 samples), DSDP Site 521 (46 samples) and ODP Sites 1264 and 1265 from the mid-latitude South Atlantic (18 samples), and ODP Site 845 from the eastern equatorial Pacific (21 samples). In these sections sampling sets with different (lower) sample resolution mainly focused on the lower distribution range of *R. pseudoumbilicus* and its relation to other concomitant biostratigraphic events.

The samples were processed following the smear-slides standard procedure described by Bown & Young (1998). Semiquantitative and morphometric analyses were carried out using a light microscope at 1200X magnification under cross-polarized and plane-transmitted light.

We evaluated the abundance distribution of *R. pseudoumbilicus* by counting the number of specimens in 30 fields of views (N/mm^2). In 39 selected samples morphometric analysis was carried out by measuring the major axis of the elliptical shape of 100 placolith specimens of *Reticulofenestra*, obtaining the relative percentages of three size-groups: small *Reticulofenestra* (major axis ≤ 4 μm in length), medium-sized *Reticulofenestra* (major axis 5-6 μm in length) and typical *R. pseudoumbilicus* (major axis ≥ 7 μm in length). Other counting was performed with biostratigraphic purpose for evaluating the partial distribution of *Discoaster signus* (= *D. petalosus*) and *Sphenolithus heteromorphus*, also expressed as N/mm^2, and *Discoaster deflandrei*, evaluated as percent (%) of all the *Discoaster* specimens observed. Morphometric analysis of images of nannofossil specimens were performed by using image analysis software "Image-pro plus 7.0".

To date the lowermost part of the sedimentary succession at Site U1338, we developed a new age model by astronomically tuning the magnetic susceptibility (MS) record in the revised composite section published by Wilkens et al. 2013. Prior to analysis, a stratigraphic gap between 393.36 and 394.69 m was partially covered by adding off-splice MS data from core U1338A-42X. The spectral analysis of the MS record was performed using the periodogram method and identified a dominant spectral frequency

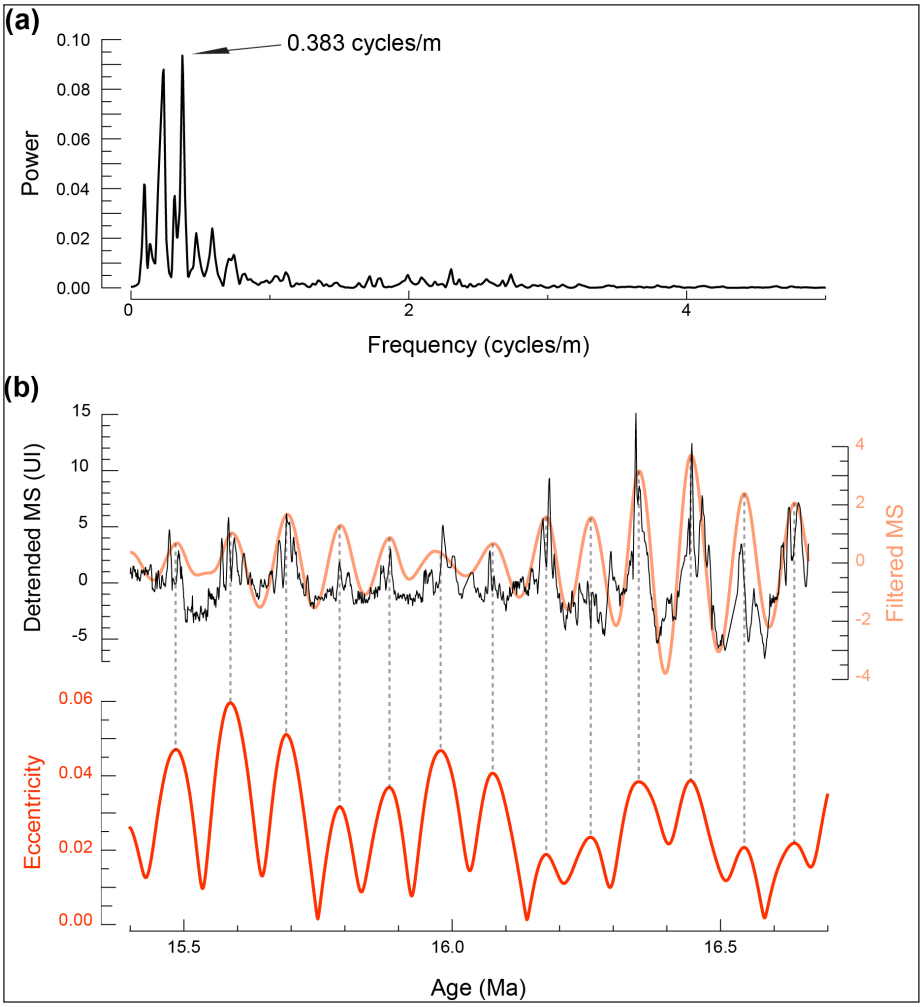

Fig. 3 - Periodogram (a) of LOWESS-detrended MS, filtered MS and eccentricity tuning target (b, Laskar et al., 2004) at Site U1338. The age model was built following two steps. Firstly, the MS record was filtered at 0.383 cycles/m, the dominant frequency of the record. High peaks in the filtered MS records were then correlated to the 100 kyr eccentricity maxima (grey dashed lines).

of ~0.383 cycles/m, which was interpreted as reflecting 100 kyr eccentricity cycles (Fig. 3). The MS record was filtered using a band-pass Gaussian filter with a frequency of 0.383 cycles/m and a bandwidth of 0.105 cycles/m. The age model was built by correlating high peaks in the MS filter to 100 kyr eccentricity maxima (Laskar et al. 2004). Orbital tuning and age calculation were performed using the AnalySeries 2.0 software (Paillard et al. 1996).

Biostratigraphy and chronology

The interval studied in detail corresponds to Zones CNM6 and CNM7 (Backman et al. 2012), equivalent to Zones NN4 (Martini 1971) and Zones CN3 and CN4 (Okada & Bukry 1980). The zonal boundary is placed at 381.54 m and corresponds to the biohorizon B *D. signus*. This biohorizon is associated with the biohorizon Top common (Tc) *D. deflandrei* that occurs slightly above, at 380.41 m. The rest of the section, down to the contact with seafloor basalt at the bottom hole in core U1338C-47H, is within the range of *S. heteromorphus* (Fig. 4). This biostratigraphic result indicates that the lowermost part of the Site U1338 succession is younger than previous results (Pälike et al. 2010; Ciummelli et al. 2017), as Bc *S. heteromorphus* has been astronomically calibrated to 17.65 Ma (Backman et al. 2012). The previously inferred age (18.40 Ma) for IODP Site U1338 terminal depth (cf. Backman et al. 2016) was based on the reconstruction of sedimentation rate history that used two biostratigraphic age-depth control points in the deepest portion of the section, namely the biohorizons B *D. signus* (15.73 Ma) and Base common (Bc) *S. heteromorphus* (17.65 Ma) (Backman et al. 2012).

The new chronology overlaps the existing astronomically tuned age model (Holbourn et al. 2014) from 377.48 to 393.53 m (Fig. 5) and dates sediment down to the lowermost core retrieved at Site U1338 (U1338C-47H), corresponding to a maximum depth of 410.52 m. This age model is consistent with the existing at Site U1338 (Holbourn et al.

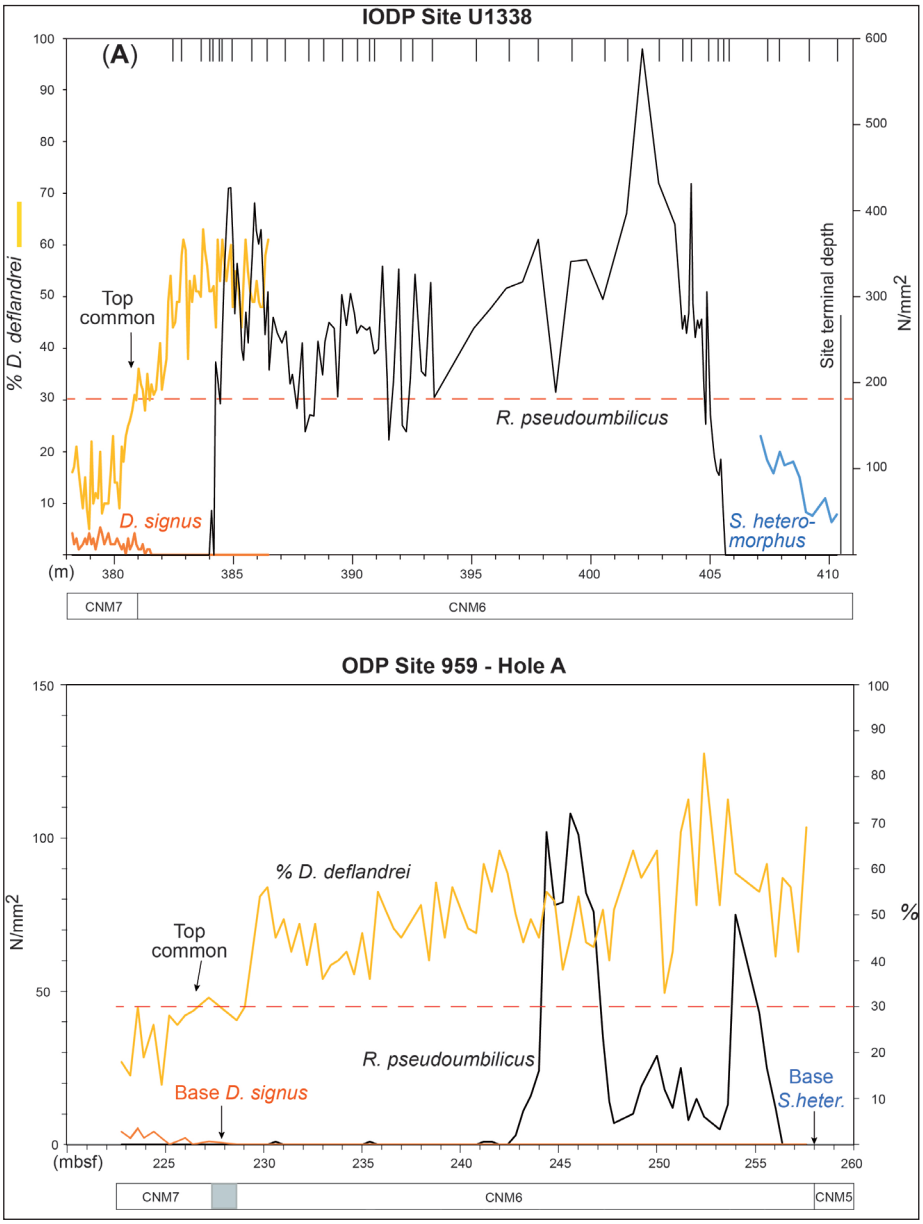

Fig. 4 - Abundance distribution pattern of *R. pseudoumbilicus* in the upper Lower Miocene interval with the partial distribution ranges of *D. deflandrei* and bottom range of *D. signus* and *S. heteromorphus* at IODP Site U1338 (Eastern equatorial Pacific) (upper panel) and ODP Site 959 (Eastern equatorial Atlantic) (lower panel). Abundance data are expressed relative to the unit area (number of specimens per square millimeter - N/mm^2) except for data on *D. deflandrei* expressed as % of *Discoaster* specimens. Biostratigraphic data are from this study with calcareous nannofossil biozones from Backman et al. 2012. Samples used for morphometry at Site U1338 are shown (**A**). Depths in m (= CCSF-B) at Site U1338, and mbsf (meter below sea floor) at Site 959.

2014; Fig. 6) and neighbouring sites (e.g., Kochhann et al. 2016, 2017). The studied interval (378.24-410.52 m) spans between 15.42 and 16.67 Ma, with average sedimentation rate of 28.6 m/Myr and ranging from 22.3 to 38.7 m/Myr. (Fig. 3). Therefore, the biomagnetostratigraphic age model proposed by Backman et al. (2016) and constructed using shipboard magnetostratigraphic data, diatom and calcareous nannofossil biostratigraphy, is unprecise and should be revised for the lowermost interval. However, some discrepancies with magnetostratigraphic data have also been highlighted during the age model building process and reveal inaccuracies in i) age models (this study and Holbourn et al. 2014), ii) age calibration of magnetostratigraphic data, or iii) a combination of both.

Results

Morphometric Analysis

Results of the morphometric analysis of *Reticulofenestra* specimens are reported in Figure 6. The selected samples are located throughout the studied interval (Fig. 4) to document the size variability within the *Reticulofenestra* population. According to the subdivision described in the "Taxonomic remarks" chapter, the three morphotypes considered show variable relative abundances at different stratigraphic levels: the clear indication of the first occurrence of *R. pseudoumbilicus* (B *R. pseudoumbilicus*) and its subsequent disappearance are evident at 405.6 m and 384.05 m respectively. The medium (5-6 μm) and small (≤ 4 μm) sized *Reticulofenestra* morphot-

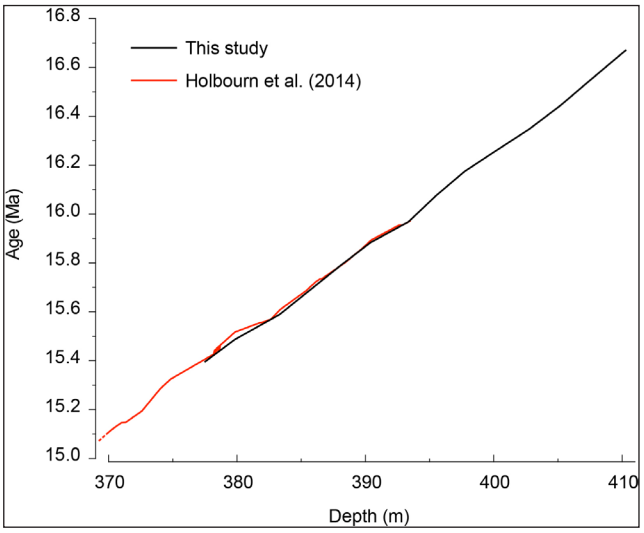

Fig. 5 - Site U1338 age models for the 370-411 m interval. Note that the two age models are very similar across the interval of overlap. Differences are <18.6 kyr between 393.53 and 381.94 m. Slightly greater discrepancies (up to 30.4 kyr) between 381.94 and 377.48 m are mainly due to different composite section used. The age model of Holbourn et al. (2014) is based on the shipboard composite section (Pälike et al. 2010), whereas the age model generated in this study is based on the revised composite section (Wilkens et al. 2013).

ypes are present in the lower part of the studied U1338 succession, the medium sized morphotypes prevail over the small morphotypes, mainly in the interval just preceding the appearance of the larger *R. pseudoumbilicus* (7-11 μm). Note that the small reticulofenestrids are recorded from the base of the Miocene (*R. haquii*) and from the middle Eocene (*R. minuta*), according to the ranges reported in Nannotax3 (https://www.mikrotax.org/Nannotax3/).

Within the lower part of its distribution range, *R. pseudoumbilicus* prevails over the other reticulofenestrids up to its temporary disappearance, labelled as "the first disappearance of *R. pseudoumbilicus* (1st disappearance *R.p.*)" (Figs. 6, 7). The small morphotypes increase in abundance in the interval just above this temporary disappearance. "First" is intended as "located in stratigraphically lower position" because this temporary disappearance of the taxon seems to precede the other similar event (here labelled as the "2nd disappearance" in Fig. 7) that occurs in the Late Miocene and delineates the beginning of the well-known "*R. pseudoumbilicus* Absence interval" (or "small *Reticulofenestra* interval"). This interval is defined by biohorizons Base absence (Ba) and Top absence (Ta) and has been globally recorded at low and mid latitude locations (e.g. Rio et al. 1990a; Gartner 1992; Young 1990; Backman & Raffi 1997; Raffi et al. 2003), as well as at IODP Site U1338 (Pälike et al. 2010).

Additional morphometric analysis performed in samples from upper stratigraphic intervals of IODP Site U1338 evidenced similar distribution patterns of the *Reticulofenestra* morphotypes in correspondence with the other appearance and temporary disappearance episodes observed (Fig. 7). In fact, comparable patterns result in these intervals: i) close to T *S. heteromorphus* in the Middle Miocene (Zone CNM7/CNM8 boundary at 327.78 m); ii) at the beginning and at the end of the Absence interval of *R. pseudoumbilicus* biohorizons in the Upper Miocene; iii) close to the final exit of *R. pseudoumbilicus* at the Lower-Upper Pliocene transition (Fig. 7).

The distribution pattern of *R. pseudoumbilicus* in the Lower Miocene

The abundance of *R. pseudoumbilicus* in the IODP Site U1338 Lower Miocene succession, between a lowermost occurrence (Base at 405.5 m) and the 1st disappearance of the taxon (at 384.05 m) is shown in Figure 4. Biostratigraphically, the depicted range of *R. pseudoumbilicus* is bracketed by the biohorizons Bc *S. heteromorphus* at the base, and B *D. signus* and Top common (Tc) *D. deflandrei* at the top (Fig. 4). The distribution appears continuous with variable abundances throughout the range, reaching a peak (~600 N/mm^2) at ~402 m. This interval with high abundance of *R. pseudoumbilicus* cannot be constrained with more detail because it occurs within a lower resolution sampling interval, between 393 and 403 m.

We compared the biohorizon B *R. pseudoumbilicus* to the tropical Atlantic ODP Site 959 succession (Mascle et al. 1996), where the stratigraphic position of the biohorizon roughly conforms with that observed in Eastern equatorial Pacific (Fig. 4) and has been recorded slightly (~1.5 m) above B *S. heteromorphus*. However, the distribution pattern of the taxon in this succession significantly differs from what we observed at IODP Site U1338 and shows variable (lower) abundances of the taxon throughout its range (Fig. 4). We also analysed the position of B *R. pseudoumbilicus* biohorizon relative to B *S. heteromorphus* biohorizon at ODP Sites 1264 and 1265 (Fig. 8). Although analysis was performed on only few samples in a not well resolved interval, it confirmed observations from Site U1338. At

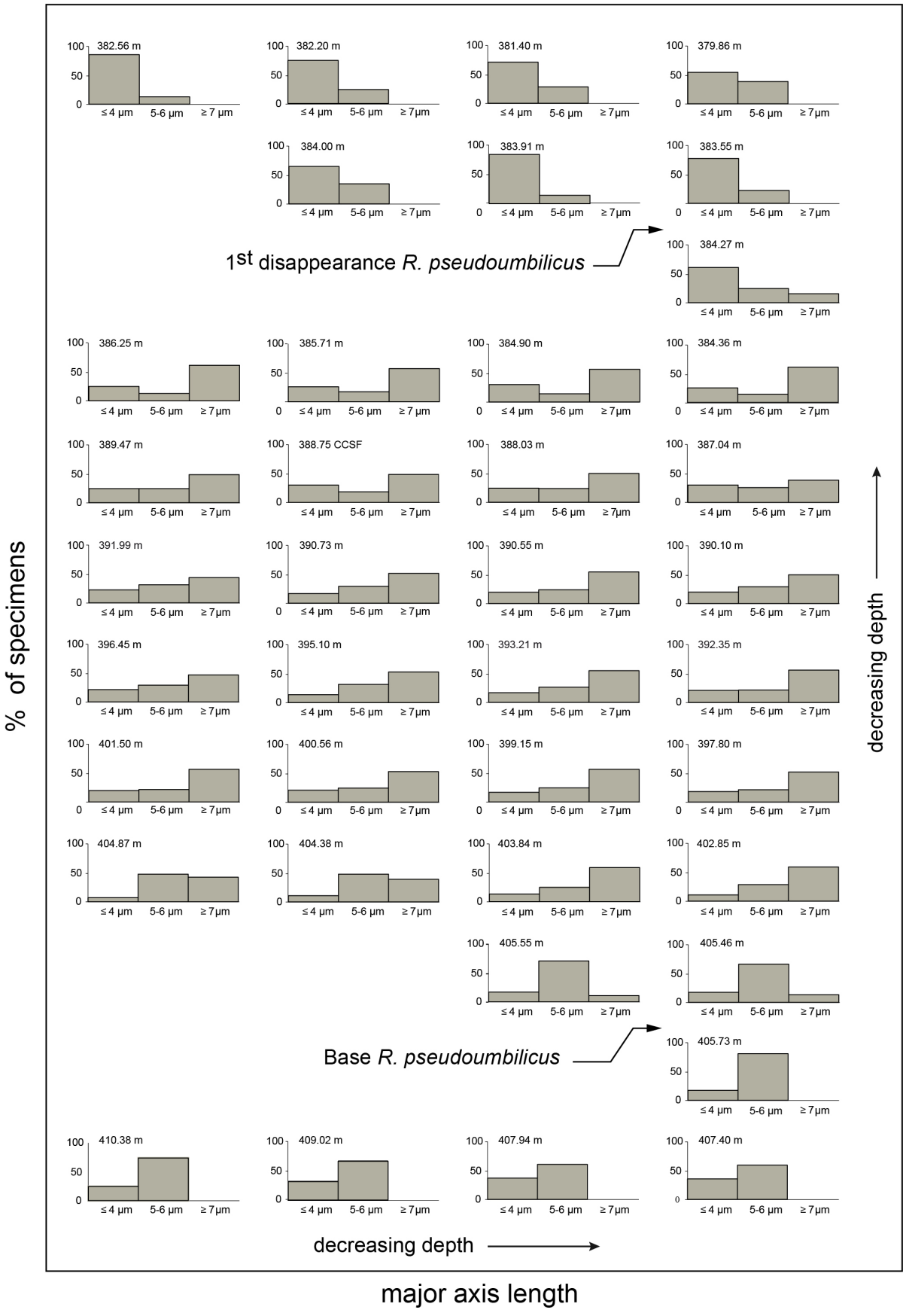

Fig. 6 - Single sample histograms of reticulofenestrids through the studied interval at Site U1338, showed in stratigraphic succession with increasing depths (m) from left to right and from bottom to top (arrows). Histograms represent relative abundances (%) of three morphogroups of *Reticulofenestra*: small-sized reticulofenestrids (≤ 4 µm in length), medium-sized reticulofenestrids (5-6 µm) and large-sized reticulofenestrids ascribed to *R. pseudoumbilicus* species (≥ 7 µm).

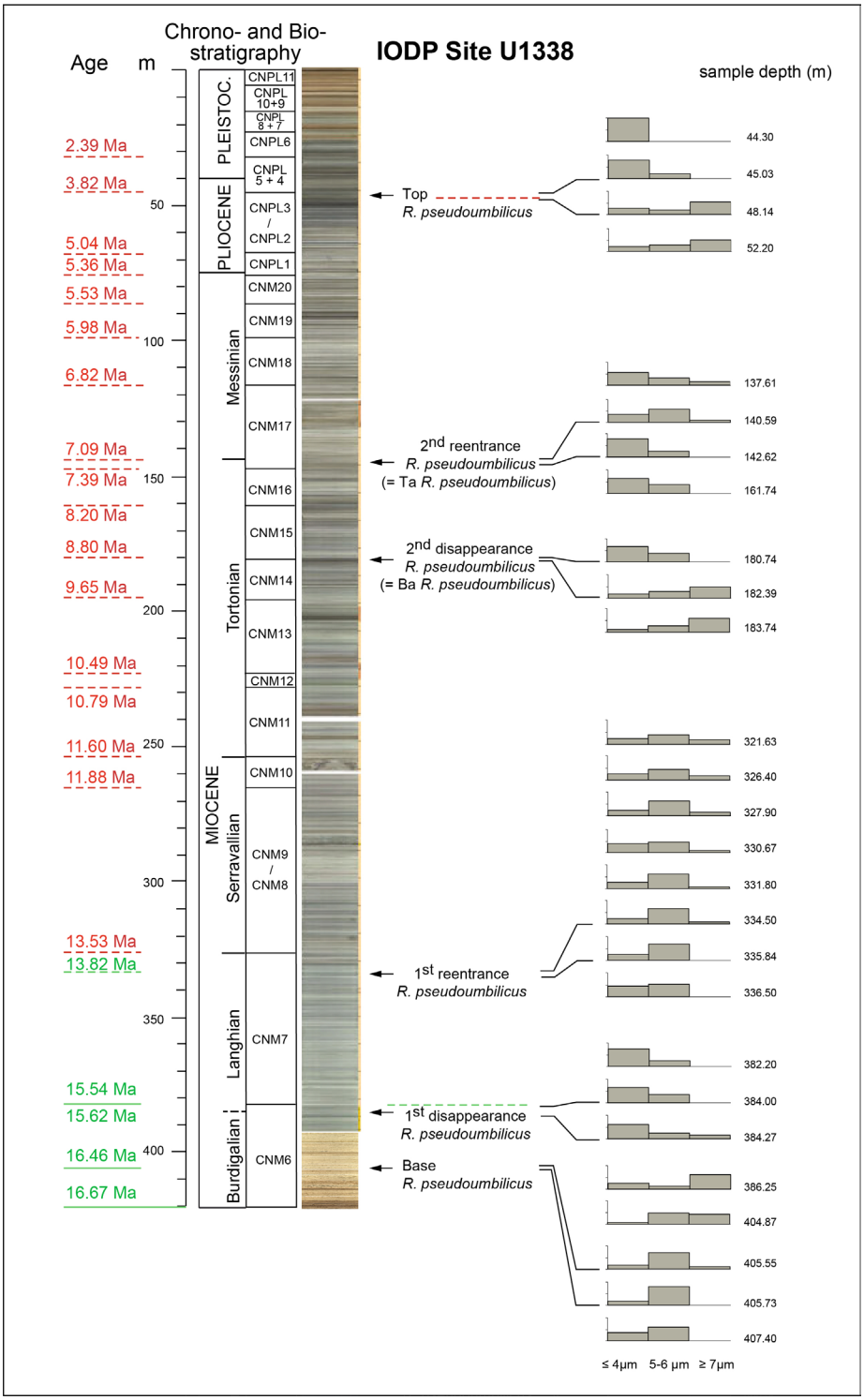

Fig. 7 - Interval of the range of *R. pseudoumbilicus* at IODP Site U1338 from the late Early Miocene to the Late Pliocene, with selected histograms through critical appearance and disappearance events of the taxon. Positions of age horizons to the left correspond to nannofossil biochronologic data from this study (green lines), and from Ciummelli et al. (2017) and Pälike et al. 2010 (red lines), referred to biohorizons reported in Table 1.

these sites the stratigraphic position of the lower range of *R. pseudoumbilicus* is bracketed between B *S. heteromorphus* and B *D. signus* plus Tc *D. deflandrei* biohorizons. This newly defined B *R. pseudoumbilicus* can be considered a useful additional biohorizon for biostratigraphic classification in the upper Lower Miocene interval.

The lowest temporary disappearance of *R. pseudoumbilicus* (1st disappearance *R.p.*) at Site U1338 precedes B *D. signus* and Tc *D. deflandrei* (by only ~3 and 3.5 m, respectively) (Fig. 4). A notably different position for the event was observed for ODP Site 959 where it is located well below (~15 m) the biohorizons B *D. signus* and Tc *D. deflandrei*. Conversely, at the other studied locations, despite the lack of high-resolution sample sets, a similar relative position to that at Site U1338 has been observed (Figs. 8, 9), with the 1st disappearance *R.p.* event occurring

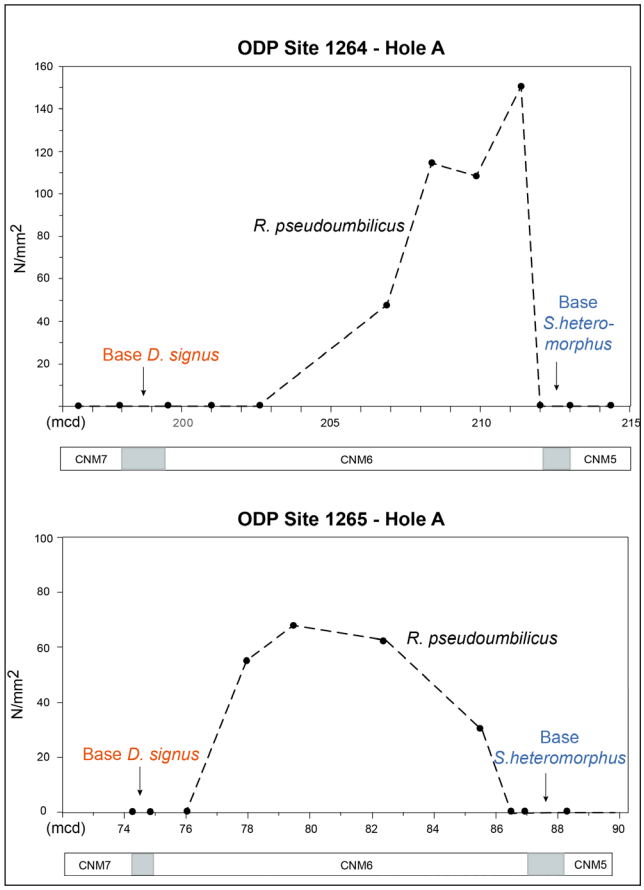

Fig. 8 - Abundance distribution pattern of *R. pseudoumbilicus* in low resolution sampling set at ODP Sites 1264 (upper panel) and 1265 (lower panel). Biostratigraphic data are from this study and ODP Leg 208 shipboard data (Zachos et al. 2004). Depths in mcd (meter composite depth). Notation as specified in Fig. 4.

below or close to B *D. signus* and Tc *D. deflandrei*. It is worth mentioning that the precise stratigraphic placement of Tc *D. deflandrei* has been quite a challenge because of the definition of the event, defined as a decrease in abundance (Bukry 1973). This biohorizon is biostratigraphically significant, because it is the prelude of a distinctive turnover in the whole *Discoaster* assemblage known to occur within the Miocene (Ciummelli et al. 2017). As previously observed for the tropical Indian, Pacific and Atlantic Oceans and the mid-latitude North and South Atlantic (e.g. Rio et al. 1990; Raffi & Flores 1995; Raffi et al. 2006), the decline of *D. deflandrei* at Site U1338 follows a gradual pattern leading to the abundance decrease that defines the biohorizon. Differences in the pattern of *D. deflandrei* decrease are observed in the studied sections that are located in different ocean basins and/or at different latitudes (Figs. 8, 9) and are likely related to local paleoceanographic conditions. Even if the influence of local conditions also explains the differences of the *R. pseudoumbilicus* distribution below the 1st disappearance event, the relative position of this event precedes B *D. signus* and Tc *D. deflandrei* in all the sections.

Discussion

The pattern of size shifts within *Reticulofenestra* in the Neogene

Our results contribute to defining the evolutionary emergence of *R. pseudoumbilicus* in the late Early Miocene and delineate the variability of its distribution pattern at different locations. Although the difference in sampling resolution for the studied sections could explain part of the observed variability, the obtained data on the appearance (Base) of *R. pseudoumbilicus* suggests a similar stratigraphic position at IODP Site U1338 and ODP Sites 959, 1264 and 1265 for this biohorizon (Fig. 10). The new age model for the lower part of the section at Site U1338 dates the B *R. pseudoumbilicus* to 16.46 Ma, the 1st disappearance R.p. to15.62 Ma and the 1st re-entrance R.p. to 13.82 Ma. Moreover, the estimated age of the marker biohorizon B *D. signus* and the associated biohorizon Tc *D. deflandrei* are 15.54 Ma and 15.50 Ma, respectively, indicating a ~0.2 Myr diachrony with the ages obtained from the reference ODP Site 925 (Ceara Rise, equatorial Atlantic; Backman et al. 2012).

The 1st disappearance *R.p.* event shows a degree of diachrony among the different sites, either at mid-latitude locations (DSDP Sites 608 and 521, northern and southern Atlantic, respectively) and at equatorial locations (ODP Sites 925 and 845, western Atlantic and eastern Pacific, respectively) (Figs. 9, 10). A relevant diachrony compared to Site U1338 data is also apparent at Site 959 (Fig. 4) and suggests that regional environmental conditions have controlled *R. pseudoumbilicus* distribution in these two sites, both located close to the Equator during the Early Miocene but in different oceanic areas, thus under different paleoceanographic regimes: IODP Site U1338 was located in the EEP northward of the narrow equatorial upwelling system (Pälike et al. 2010), and ODP Site 959 in an eastern Atlantic area characterized by variable upwelling related to monsoon variability (Mascle et al. 1996; Wagner 2002).

Although the distribution patterns observed in the lower part of the documented ranges differ,

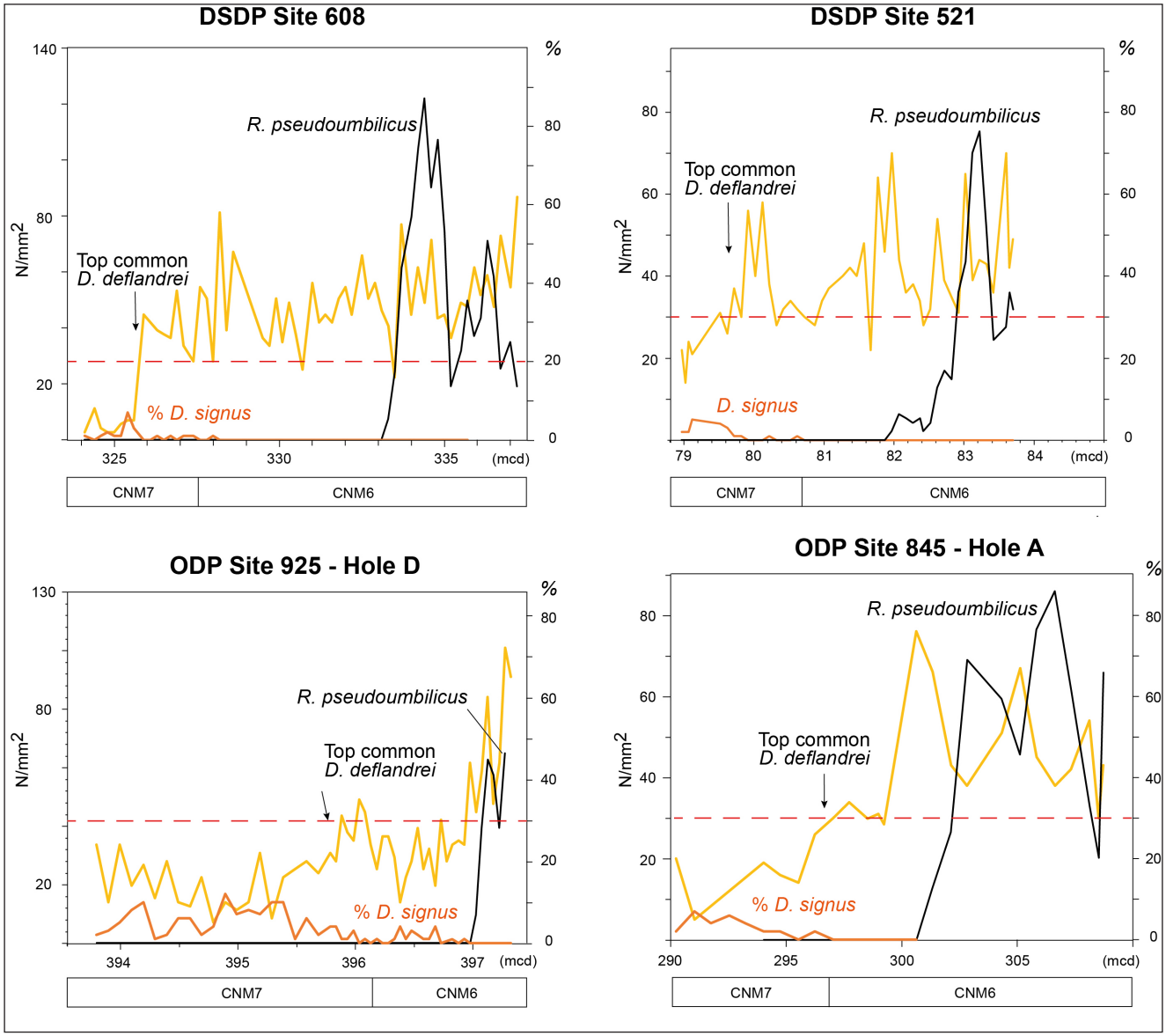

Fig. 9 - The stratigraphic position of the "1st disappearance of *R. pseudoumbilicus*" relative to the uppermost distribution range of *D. deflandrei* and lowermost distribution range of *D. signus* at mid-latitude ODP Sites 608 and 521 (North Atlantic and South Atlantic, respectively) (upper panel), and at low latitude ODP Sites 925 and 845 (equatorial Atlantic and Eastern equatorial Pacific, respectively) (lower panel). Biostratigraphic data are from this study.

the evolutionary emergence of *R. pseudoumbilicus* is clearly delineated. This event results from a pattern of size increase within *Reticulofenestra,* a taxon that has been present in the stratigraphic record since the lower Eocene (Ypresian) with species included within the *R. pseudoumbilicus* group and *R. umbilicus* group (cf. Nannotax3-ntax_cenozoic-Microtax). Specifically, *R. pseudoumbilicus* evolved from small size *Reticulofenestra* specimens (ascribed to the species *R. haqii*) and its evolutionary emergence represents one of the various size increase episodes within reticulofenestrid placoliths observed throughout a lineage that spans more than 50 Myr. In the literature, there is no documented evolutionary relationship between *R. pseudoumbilicus* and the species *Reticulofenestra dictyoda* or *Reticulofenestra daviesii*, taxa with similar size and outline that evolved in the early Eocene (Ypresian) and in the middle Eocene (Lutetian) respectively, were common in the late Eocene and Oligocene and gradually disappeared from the stratigraphic record in the earliest Miocene. The appearance of *R. pseudoumbilicus* can be explained as the result of i) size increase in an existing species (*R. haqii*), or ii) a new species radiation expressed by a distinct size increa-

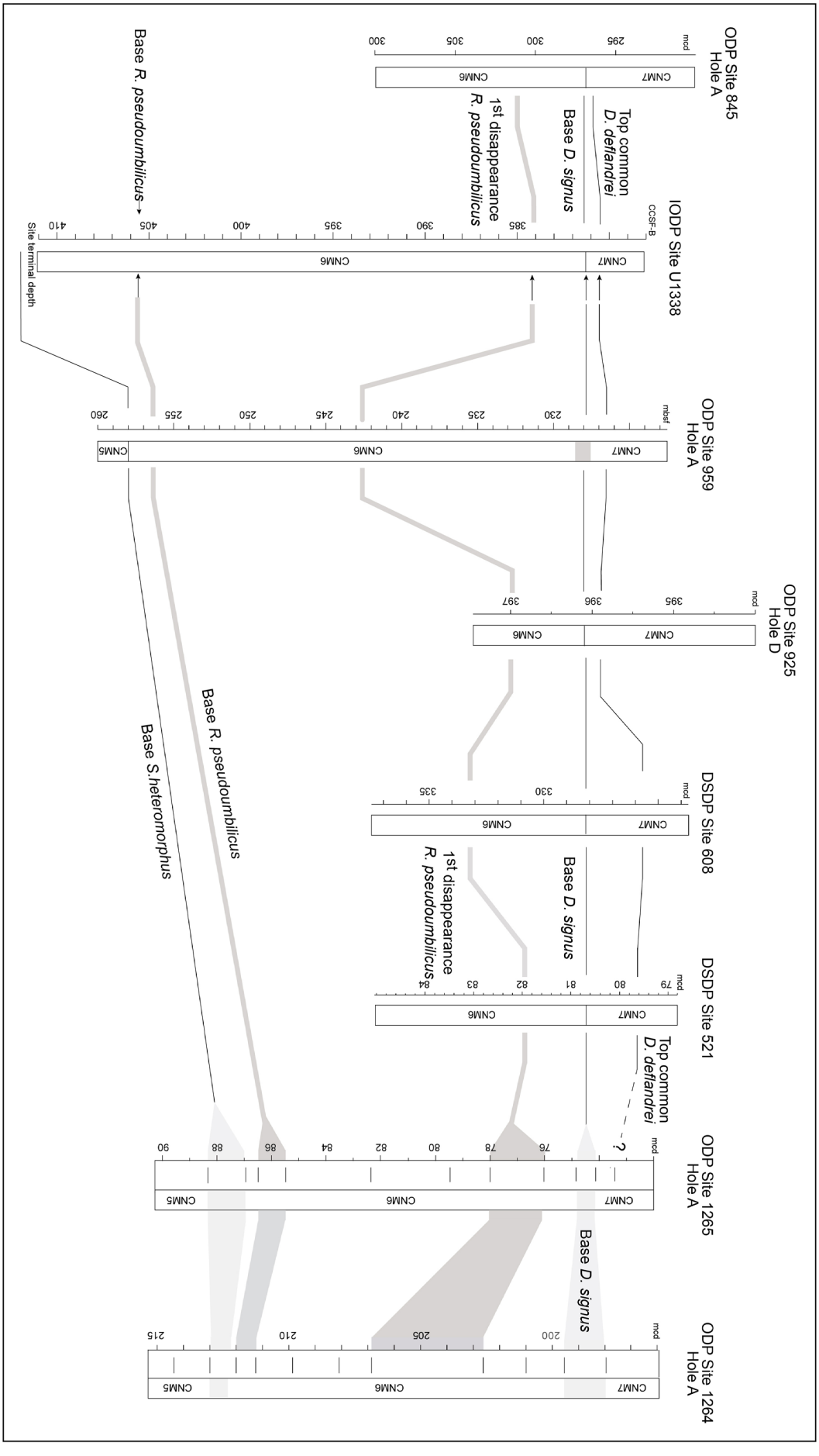

Fig. 10 - The stratigraphic position of the Early Miocene biohorizons related to *R. pseudoumbilicus* distribution in the studied successions located in the eastern equatorial Pacific (IODP Site U1338 and ODP Site 845), the eastern and western equatorial Atlantic (ODP Sites 959 and 925, respectively), the mid-latitude North (DSDP Site 608) and South (DSDP Site 521, ODP Sites 1264 and 1265) Atlantic oceans.

se, without other relevant changes in morphology, from an ancestral species *R. haqii*.

The documented episode of temporary exit of this new species (1st disappearance *R.p.*) from the stratigraphic record after its evolutionary emergence replicates the pattern observed in the distribution range of *R. pseudoumbilicus* in upper stratigraphic intervals at Site U1338 (Fig. 7). Although the episodes of re-entrance and temporary disappearance of *R. pseudoumbilicus* recorded in the Upper Miocene through Pliocene interval do not have the same detailed (high resolution) documentation as in the Lower Miocene, it is possible to broadly compare the events with the climatic - environmental evolution over that time interval, with the aim of understanding the delineated pattern of size shifts within *Reticulofenestra* from an evolutionary and/or environmental point of view.

R. pseudoumbilicus size shifts vs. Neogene climatic - environmental evolution

Comparison of *R. pseudoumbilicus* evolutionary steps at Site U1338 succession (Miocene to Pliocene time interval) with benthic foraminifera stable isotopes (Westerhold et al. 2020) provides information on their linkages to global climate and carbon cycling changes. This comparison to benthic foraminifera $\delta^{18}O$ and $\delta^{13}C$ records (Westerhold et al. 2020) is based on the ages of nannofossil biohorizons from this study and Ciummelli et al. (2017) and Pälike et al. (2010) (Table 1; Figs. 11, 12).

B *R. pseudoumbilicus* is documented within a warm climate period marked by low $\delta^{18}O$ peak within the Miocene Climatic Optimum (MCO). Recorded "re-appearances" (1st and 2nd re-entrances *R.p.*) correspond to intervals of global climate cooling (Fig. 11). They respectively occur during the Middle Miocene Climatic Transition (MMCT) toward a phase of Antarctic ice-sheet expansion, and close to the onset of Late Miocene Cooling (LMC). An interesting observation results from comparison of these Neogene events with the distribution pattern of the reticulofenestrids in the early and middle Eocene, namely the small sized *Reticulofenestra minuta* and the medium/large sized *R. dictyoda* and *R. daviesii* (belonging to *R. pseudoumbilicus* group, *R. umbilicus* and *R. lockeri* group, respectively; cf. Nannotax3). In fact, these Paleogene reticulofenestrids evolved during a warm interval (the Early Eocene Climatic Optimum – EECO) but the medium/large *R. dictyoda* and *R. daviesii* successively rose in abundance and spread during a cooling phase in the late early Eocene (after 49 Ma). Subsequently, *Reticulofenestra* became dominant in the nannofossil assemblages (Agnini et al. 2006; Cappelli et al. 2019). This indicates that both the Neogene and Eocene *Reticulofenestra* taxa evolved during warm time intervals and show a similar trend of increased size in species/specimens and expansion within nannofossil assemblages during climate cooling, in line with the environmental preferences (temperate and mesoeutrophic) established for *Reticulofenestra* (e.g., Villa et al. 2008; Cappelli et al. 2019).

The recorded "disappearances", namely 1st and 2nd disappearance *R.p.* and T *R. pseudoumbilicus*, occur during warmer climate conditions (Fig. 11). The 1st disappearance *R.p.*, occurs at the climax of the MCO at ~15.6 Ma (Holbourn et al. 2015; Kochhann et al. 2016; 2017). The 2nd disappearance *R.p.* occurs at the beginning of a negative $\delta^{18}O$ shift at ~8.8 Ma. T *R. pseudoumbilicus* biohorizon is located at the beginning of the ~0.3 Ma negative $\delta^{18}O$ shift of the PCO (Pliocene Climatic Optimum).

Comparing the distribution of *R. pseudoumbilicus* with the benthic foraminifera $\delta^{13}C$ record (Westerhold et al. 2020), some observation can be made. Both the recorded "appearances" and "disappearances" events correlate with some of the features of the $\delta^{13}C$ record representing changes in the ocean carbon cycle (see Steinthorsdottir et al. 2021 for an overview). At Site U1338 all appearances occur during intervals of decreasing $\delta^{13}C$ (Fig. 12). B *R. pseudoumbilicus* and 1st reentrance *R.p.* correspond to two intervals of decreasing $\delta^{13}C$ within the Monterey carbon isotope excursion (MCIE) (Vincent & Berger 1985), namely below the Carbon Maxima CM-2 and CM-6 (Sosdian et al. 2020), respectively (Fig. 12). Perhaps more evident is the 2nd re-entrance *R.p.*, which occurs during the late Miocene carbon isotope shift (LMCIS), a ~1‰ decrease of the benthic $\delta^{13}C$ between ~7.7 and 6.6 Ma (Tian et al. 2018). The 1st disappearance *R.p.* is linked to the CM-3 (Carbon Maximum 3; Sosdian et al. 2020) $\delta^{13}C$ peak of the MCIE (Fig. 12). Across the MCIE, *R. pseudoumbilicus* shows a pattern of repeated events after its entrance in the stratigraphic record: it first appears, temporarily disappears and then re-enters. The correlation between this evolutionary pattern and benthic $\delta^{13}C$ suggests a relationship with global carbon cycling. Carbon maxima within the MCIE have been inter-

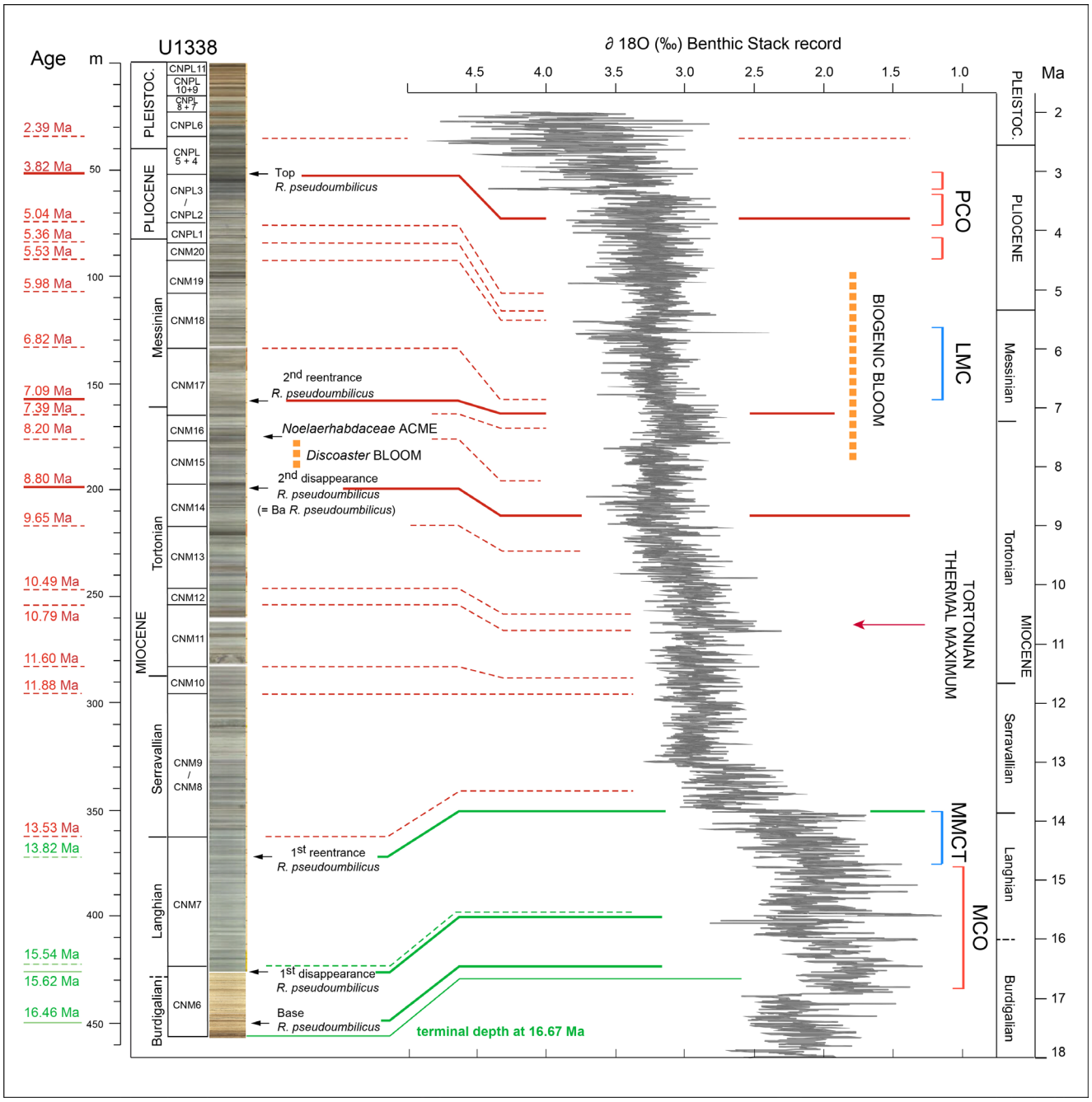

Fig. 11 - The appearance and disappearance events of *R. pseudoumbilicus* at Site U1338 succession (Miocene to Pliocene time interval) compared to benthic foraminifera $\delta^{18}O$ record (Westerhold et al. 2020). Neogene different phases of low, increasing in and high $\delta^{18}O$ are reported: MCO = Miocene Climatic Optimum; MMCT = Middle Miocene Climatic Transition; LMC = Late Miocene Cooling; PCO = Pliocene Climatic Optimum. Positions of age horizons to the left correspond to nannofossil biochronology from this study (green lines), and from Ciummelli et al. (2017) and Pälike et al. (2010) (red lines), referred to biohorizons reported in Table 1. Other events within nannofossil assemblages in the late Tortonian are also reported to the left (*Discoaster* BLOOM, from Ciummelli et al. 2017; Noëlaerhabdaceae ACME, from Beltran et al. 2014).

preted as reflecting intervals of increased marine productivity compared to intervals of lower $\delta^{13}C$ (Tian et al. 2018; Sosdian et al. 2020; Steinthorsdottir et al. 2021). Following this rationale, in the early-middle Miocene *Reticulofenestra* size increase events occurred during intervals of decreased productivity, whereas size decrease events occurred during intervals of increased productivity. The 2nd disappearance *R.p.* occurs in correspondence to a high $\delta^{13}C$ peak at the end of the Carbonate Crash (~11 - 8 Ma; Lyle et al. 1995) and the subsequent interval of absence in the Late Miocene has been found in different ocean

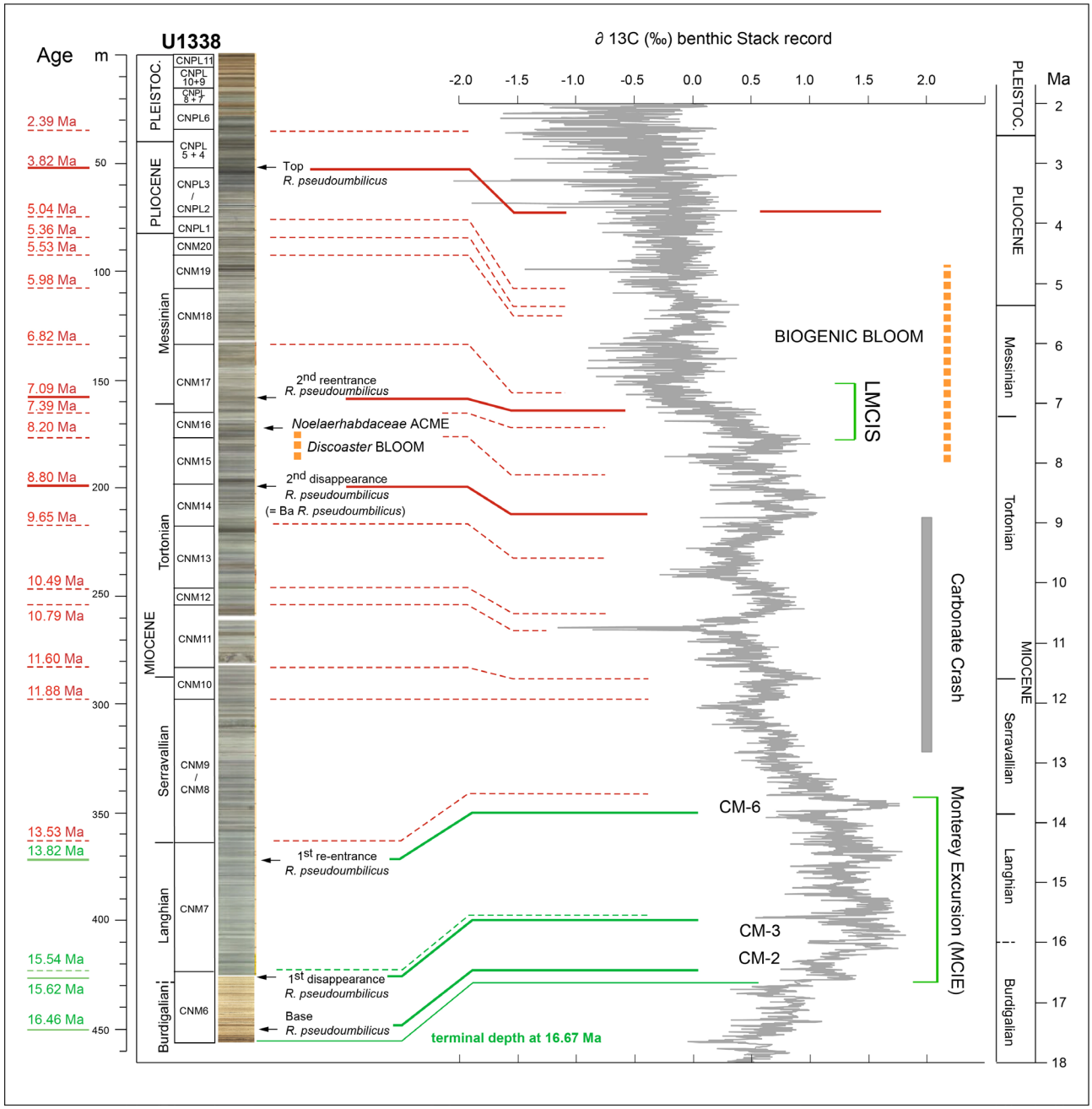

Fig. 12 - The appearance and disappearance events of *R. pseudoumbilicus* at Site U1338 succession (Miocene to Pliocene time interval) compared to benthic foraminifera $\delta^{13}C$ record (Westerhold et al. 2020). Neogene different carbon cycle perturbations are reported: Monterey Excursion (MCIE); carbon isotope maxima CM-2, CM-3 and CM-6; Carbonate Crash; Biogenic Bloom; LMCIS = Late Miocene Carbon Isotope Shift. Other notation as specified in Fig. 12.

basins and represents a widespread biostratigraphic signal with a well constrained age between 8.8 and ~7.1 Ma. This absence interval terminates within the "Biogenic bloom", a widespread increase in primary production (Diester-Haas et al. 2006; Reghellin et al. 2020; 2022), and toward the end of the LMCIS. It is worth noting that at Site U1338, within this Late Miocene absence interval of *R. pseudoumbilicus,* a discoasterids bloom (Ciummelli et al. 2017) and an acme of opportunistic small (< 3 μm) reticulofenestrid-type placoliths (Beltran et al. 2014) occurred. Multiproxy data indicate that the 100 kyr-long acme occurred in warm surface waters, with a deep thermocline and low nutrient supply and was related to external forcing (low-eccentricity and low-insolation at the Equator; Beltran et al. 2014).

Although the correlation to benthic $\delta^{13}C$ is less obvious compared to the other two disappea-

ZONE (base)	BIOHORIZON	AGE (Ma)	m (CCSF-B)
CNPL6	**T** *D. pentaradiatus*	2.39	32.50
CNPL4	**T** *R. pseudoumbilicus*	3.82	46.81
CNPL2	**T** *C. acutus*	5.04	68.14
CNPL1	**B** *C. acutus*	5.36	76.35
CNM20	**T** *D. quinqueramus*	5.53	83.71
CNM19	**T** *N. amplificus*	5.98	96.85
CNM18	**B** *N. amplificus*	6.82	117.83
CNM17	**2nd reentrance** *R. pseudoumbilicus*	7.09	143.22
	B *A. primus*	7.39	147.98
CNM16	**B** *D. berggrenii*	8.20	160.29
CNM15	**2nd disappearance** *R. pseudoumbilicus*	8.80	180.09
CNM14	**T** *D. hamatus*	9.65	195.79
CNM13	**B** *D. hamatus*	10.49	222.26
CNM12	**B** *C. coalitus*	10.79	228.84
CNM11	**Tc** *D. kugleri*	11.60	253.46
CNM10	**Bc** *D. kugleri*	11.88	265.50
CNM8	**T** *S. heteromorphus*	13.53	325.93
CNM7	***1st reentrance*** *R. pseudoumbilicus*	*13.82*	*335.15*
	Tc *D. deflandrei*	*15.5*	*380.41*
	B *D. signus*	*15.54*	*381.54*
	1st disappearance *R. pseudoumbilicus*	*15.62*	*384.13*
	B *R. pseudoumbilicus*	*16.46*	*405.60*

Tab. 1 - Calcareous nannofossil biohorizons at IODP Site U1338 succession, with depth position and ages. Data and ages from this study are in *Italic*, other data are from Ciummelli et al. (2017) and Pälike et al. 2010 with biochronology from Backman et al. 2012.

rance events, T *R. pseudoumbilicus* does occur during an interval of relatively high $\delta^{13}C$ during the Pliocene. Analogously to what we observed in the comparison to $\delta^{18}O$ record, the correlation between the reticulofenestrids distribution pattern and benthic $\delta^{13}C$ record in the Neogene seems to be similar to what observed for the Paleogene reticulofenestrids (Cappelli et al. 2019).

Possible mechanisms of size changes within reticulofenestrids.

In general, the observed pattern reflects the previous reconstructions of reticulofenestrids size variation during the Middle Miocene-Pliocene (Young 1990) and the abundance pattern in the middle Miocene climatic transition (Henderiks et al. 2020), that recorded marked diversification in size and abundance variability. The temporary absence of larger reticulofenestrids starting from ~8.5 Ma, documented by Young (1990), and their presence starting from ~13.8 Ma (above the MMCT; Henderiks et al. 2020) are in agreement with our data. The new finding about the evolutionary emergence of large *R. pseudoumbilicus,* in a stratigraphic interval older than previously recorded, only adds another detail in the peculiar pattern of distribution of the taxon through the Neogene. This pattern reflects similar stepwise variability in size observed in other nannoplankton/nannofossils, such as the pattern of size changes showed by the genus *Gephyrocapsa* (Rio 1982; Matsuoka & Okada 1990; Raffi et al. 1993), another taxon belonging to the Noëlaerhabdaceae family. This macroevolutionary pattern of recurrent size increase/decrease events observed in the Pliocene-Pleistocene, that have been convincingly interpreted as the result of repeated species radiations and extinctions within the *Gephyrocapsa* lineage and supported by genomic analyses of extant species (Bendif et al. 2019). Moreover, these authors suggested that the *Gephyrocapsa* macroevolutionary events were climatically sensitive and appeared as a response to the step changes in global cooling, typical of the Pleistocene interval. Hence, the repeated episodes of size increase and size reduction, (appearance and disappearance of *R. pseudoumbilicus*, respectively), documented in this study within the Neogene *Reticulofenestra*, share with other coccolithophores, *Gephyrocapsa* in the Quaternary and reticulofenestrids in the Paleogene, the common feature of occurring concomitantly with step changes toward cooler conditions.

As opposed to the results obtained on the *Gephyrocapsa* lineage by Bendif et al. (2019), the data from the present study leave doubts on the interpretation of the observed recurrent size changes of *Reticulofenestra*. Namely, they could represent i) events of speciation followed by extinctions or could cor-

respond to fluctuation in abundance of the new species *R. pseudoumbilicus* or ii) changes in the relative abundance of large- and small specimens of a species that already existed, as *R. haqii*. The fact that individual coccospheres can bear coccoliths with highly different sizes and the coccolith size variability can be in part related to environmental perturbation (Suchéras-Marx et al. 2022, and references therein) supports the latter interpretation.

The observed repeated events correspond to size shifts of specimens that do not show other morphologic change at any "reappearance" (cf. Fig. 2). Therefore, the similarity of the large *R. pseudoumbilicus* specimens observed both in Miocene and Pliocene intervals could suggest that the repeated pattern of size increase, interspersed between intervals with only small specimens, does not represent repeated episodes of species radiation. Instead, the described pattern could reflect an ecophenotypic response to changing paleoenvironmental factors. On the other hand, each recurrent occurrence of the large *R. pseudoumbilicus* at stratigraphically distinct intervals could be the result of a more significant evolutionary event (major species radiation), even if it was macroscopically expressed only by a simple size increase, and could represent an example of iterative evolution. The repeated evolutionary events, occurring in a portion of the *Reticulofenestra* lineage throughout the Neogene, could have been influenced by complex external factors related to climatic and environmental conditions, quite dynamic during the Miocene, and by biotic processes, such as the competition within other coccolithophore taxa.

Conclusive remarks

The appearance in the stratigraphic record of the species *R. pseudoumbilicus* in the late Early Miocene (upper Burdigalian stage), calibrated at ~16.5 Ma in the IODP Site U1338 succession, represents a new finding for calcareous nannofossil biostratigraphy, considering that this biohorizon was previously attributed to an uncertain stratigraphic position between 18.0-13.5 Ma. This appearance seems isochronous at other low and mid-latitudes locations in the Atlantic Ocean. High resolution analysis of sediment cores from IODP Site U1338 show that the distribution pattern of *R. pseudoumbilicus* after its evolutionary emergence is characterized by a temporary disappearance of the taxon (1st disappearance *R.p.*), occurring ~0.8 Myr after its lowest appearance. The beginning of this interval of absence appears to be a diachronous event based on preliminary results from comparison at different locations. This pattern of "entrance followed by temporary exit" is similar to that observed in the upper part of the taxon stratigraphic range. In fact, *R. pseudoumbilicus* re-enters two times in the stratigraphic record after two intervals of temporary disappearance lasting ~3.0 and ~4.8 Myr, respectively. These results are in line with previous reconstructions, at lower stratigraphic resolution, of reticulofenestrids diversification in size and abundance during the middle Miocene to Pliocene (Young 1990; Henderiks et al. 2020). It is not possible to unquestionably demonstrate if the pattern of repeated changes in size represents i) fluctuation in abundance of larger morphotypes of the same species *R. haqii*, ii) fluctuation in abundance of a new species, *R. pseudoumbilicus*, evolved from the ancestral species *R. haqii*, or iii) repeated episodes of species radiation within the *Reticulofenestra* lineage. Influence of environmental factors is reasonably inferred for each of the listed options.

The astronomically tuned age model presented here dates the lowermost sediment retrieved from Site U1338 to 16.67 Ma. This chronology was intentionally built to be consistent with published age models based on lower Miocene sediments from the EEP (Holbourn et al. 2014; Kochhann et al. 2016, 2017). However, inconsistencies with bio- and magneto-stratigraphic data from Site U1338 (Wilkens et al. 2013; Backman et al. 2016) suggest imprecisions in the astronomically tuned age models (this study, Holbourn et al. 2014), which therefore need to be further refined. As such, we suggest that caution should be taken when interpreting data based on these chronologies.

Comparison of *R. pseudoumbilicus* events to the benthic $\delta^{18}O$ record suggests that re-entrances of the taxon occur in correspondence with step changes in global cooling, whereas disappearances occur during global climate warming. Therefore, the *R. pseudoumbilicus* pattern can be considered another example of the recurring role played by climatic/environmental factors on evolutionary pulses of planktonic organisms (Bendif et al. 2019, and reference therein). Some of these events, e.g. B *R. pseudoumbilicus* and 2nd disappearance *R.p.*, do not seem

to follow the same pattern of the other re-entrance and disappearance events of the species, respectively (see related discussion above). This might relate to the fact that benthic foraminifera stable isotopes are not direct indicators of water properties in the ocean surface at Site U1338, where *R. pseudoumbilicus* dwelled. Comparison to proxies of surface ocean water properties is hence required in the effort to understanding the relationship between *R. pseudoumbilicus* evolutionary steps and climate/environmental conditions. Comparison to preliminary, low resolution, $\delta^{18}O$ and $\delta^{13}C$ records at Site U1338, which primarily reflect surface water temperature and biological production (Reghellin et al. 2020), generally confirms the relationship between *R. pseudoumbilicus* appearances and disappearances and benthic foraminifera stable isotopes. This statement could be clarified and confirmed by further comparison to more resolved bulk isotope records when they will be available.

Acknowledgments: We are grateful to Denise Kulhanek and an anonymous for they constructive comments that improved the text, and to Simone Galeotti for fruitful discussion on the developed age model. This research used samples provided by the Integrated Ocean Drilling Program (IODP) sponsored by the U.S. National Science Foundation (NSF) and participating countries under management of Joint Oceanographic Institutions (JOI). Research had the financial support from Università degli Studi "G. d'Annunzio" di Chieti-Pescara (AN, IR) and Università degli Studi di Urbino "Carlo Bo" (DR). Data to this article will be archived in the PANGAEA database.

References

Agnini C., Muttoni G., Kent D. V. & Rio D. (2006) - Eocene biostratigraphy and magnetic stratigraphy from Possagno, Italy: The calcareous nannofossil response to climate variability. *Earth and Planetary Science Letters*, 241(3–4): 815-830. https://doi.org/10.1016/j.epsl.2005.11.005.

Backman J. & Shackleton N.J. (1983) - Quantitative biochronology of Pliocene and early Pleistocene calcareous nannofossils from the Atlantic, Indian and Pacific oceans. *Marine Micropaleontology*, 8(2): 141-170.

Backman J. & Raffi I. (1997) - Calibration of Miocene nannofossil events to orbitally tuned cyclostratigraphies from Ceara Rise. In: Shackleton N.J., Curry W.B., Richter C. and Bralower T.J. (Eds.) - *Ocean Drilling Program Scientific Results,* 154: 83-99. College Station, TX (Ocean Drilling Program).

Backman J., Raffi I., Rio D., Fornaciari E. & Pälike H. (2012) - Biozonation and biochronology of Miocene through Pleistocene calcareous nannofossils from low and middle latitudes. *Newsletters on Stratigraphy*, 45(3): 221–244. doi.org/10.1127/0078-0421/2012/0022.

Backman J., Baldauf J.G., Ciummelli M. & Raffi I. (2016) - Data report: a revised biomagnetostratigraphic age model for Site U1338, IODP Expedition 320/32. In: Pälike H., Lyle M., Nishi H., Raffi I., Gamage K. Klaus A. & the Expedition 320/321 Scientists (Eds) - *Proceedings of the Integrated Ocean Drilling Program*, 320/321: Tokyo (Integrated Ocean Drilling Program Management International, Inc.). doi: 10.2204/iodp.proc.320321.219.2016.

Beltran C., Rousselle G., Backman J., Wade B.S. & Sicre M.A. (2014) - Paleoenvironmental conditions for the development of calcareous nannofossil acme during the late Miocene in the eastern equatorial Pacific. *Paleoceanography*, 29. doi:10.1002/2013PA002506

Bendif E.M., Nevado B., Wong E.L.Y., Hagino K., Probert I., Young J.R., Rickaby R.E.M. & Filatov D.A. (2019) - Repeated species radiations in the recent evolution of the key marine phytoplankton lineage *Gephyrocapsa*. *Nature Communications*, 10(1): 1-9. doi.org/10.1038/s41467-019-12169-7

Bown P.R. & Young J.R. (1998) - Techniques. In: Bown P.R. (Ed.) - Calcareous Nannofossil Biostratigraphy: 16-29. Kluwer Academic, Dordrecht.

Bukry D. (1973) - Low-latitude coccolith biostratigraphic zonation. In: Edgar N.T. & Saunders J.B. (Eds) - *Initial Reports of the Deep Sea Drilling Project*, 15: 685–703. Washington, DC (US Government Printing Office).

Cappelli C., Bown P.R., Westerhold T., Bohaty S.M., de Riu M., Lobba V., Yamamoto Y. & Agnini C. (2019) - The Early to Middle Eocene Transition: an integrated calcareous nannofossil and stable isotope record from the Northwest Atlantic Ocean (Integrated Ocean Drilling Program Site U1410). *Paleoceanography and Paleoclimatology*, 34(12): 1913-1930. doi.org/10.1029/2019PA003686.

Ciummelli M., Raffi I. & Backman J. (2017) - Biostratigraphy and evolution of Miocene *Discoaster* spp. from IODP Site U1338 in the equatorial Pacific Ocean. *Journal of Micropalaeontology*, 36: 137-152. doi.org/10.1144/jmpaleo2015-034

Diester-Haass L., Billups K. & Emeis K.C. (2006) - Late Miocene carbon isotope records and marine biological productivity: was there a (dusty) link? *Paleoceanography*, 21(4): 1-18. doi.org/10.1029/2006PA001267.

Drury A.J., Westerhold T., Frederichs T., Tian J., Wilkens R., Channell J.E.T., Evans H., John C.M., Lyle M. & Röhl U. (2017) - Late Miocene climate and time scale reconciliation: accurate orbital calibration from a deep-sea perspective. *Earth and Planetary Science Letters*, 475: 254-266. doi:10.1016/j.epsl.2017.07.038.

Foresi L.M., Baldassini N., Sagnotti L., Lirer F., Di Stefano A., Caricchi C., Verducci M., Salvatorini G. & Mazzei R. (2014) - Integrated stratigraphy of St. Thomas section (Malta Island): a reference section for the lower Burdigalian of the Mediterranean Region. *Marine Micropaleontology*, 111: 66-89. http://dx.doi.org/10.1016/j.marmicro.2014.06.004

Fornaciari E., Backman J. & Rio D. (1993) - Quantitative distribution patterns of selected Lower to Middle Miocene

calcareous nannofossils from the Ontong Java Plateau. In: Berger W.H., Kroenke L.W., Mayer L.A. et al. (Eds) - *Ocean Drilling Program Scientific Results*, 130: 245-256. College Station, TX (Ocean Drilling Program).

Gartner S. (1969) - Correlation of Neogene planktonic foraminifera and calcareous nannofossil zones. *Transactions of the Gulf-Coast Association of Geological Societies*, 19: 585-599.

Gartner S. (1992) - Miocene nannofossil chronology in the North Atlantic, DSDP Site 608. *Marine Micropaleontology*, 18: 307-331.

Henderiks J., Bartol M., Pige N., Karatsolis B.T. & Lougheed B.C. (2020) - Shifts in phytoplankton composition and stepwise climate change during the Middle Miocene. *Paleoceanography and Paleoclimatology*, 35(8): 1-18. doi.org/10.1029/2020PA003915

Holbourn A., Kuhnt W., Lyle M., Schneider L., Romero O. & Andersen N. (2014) - Middle Miocene climate cooling linked to intensification of eastern equatorial Pacific upwelling. *Geology*, 41(1): 19-22. doi.org/10.1130/G34890.1

Holbourn A., Kuhnt W., Kochhann K.G.D., Andersen N. & Sebastian Meier K.J. (2015) - Global perturbation of the carbon cycle at the onset of the Miocene Climatic Optimum. *Geology*, 43(2): 123-126. doi.org/10.1130/G36317.1

Kochhann K.G.D., Holbourn A., Kuhnt W., Channell J.E.T., Lyle M., Shackford J.K., Wilkens R.H. & Andersen N. (2016) - Eccentricity pacing of eastern equatorial Pacific carbonate dissolution cycles during the Miocene Climatic Optimum. *Paleoceanography*, 31(9): 1176-1192. doi.org/10.1002/2016PA002988

Kochhann K.G.D., Holbourn A., Kuhnt W. & Xu J. (2017) - Eastern equatorial Pacific benthic foraminiferal distribution and deep water temperature changes during the early to middle Miocene. *Marine Micropaleontology*, 133: 28-39. doi: 10.1016/j.marmicro.2017.05.002.

Laskar J., Robutel P., Joutel F., Gastineau M., Correia A.C.M. & Levrard B. (2004) - A long-term numerical solution for the insolation quantities of the Earth. *Astronomy and Astrophysics*, 428(1): 261-285. doi.org/10.1051/0004-6361:20041335.

Lyle M., Dadey K. & Farrell J. (1995) - The Late Miocene (11-8 Ma) eastern Pacific carbonate crash: Evidence for reorganization of deep-water circulation by the closure of the Panama Gateway. *Ocean Drilling Program Scientific Results*, 138: 821-837.

Lyle M., Pälike H., Nishi H., Raffi I., Gamage K., Klaus A. & the IODP Expeditions 320/321 Scientific Party (2010) - The Pacific Equatorial Age Transect, IODP Expeditions 320 and 321: Building a 50-Million-Year-Long Environmental Record of the Equatorial Pacific Ocean, *Scientific Drilling*, 9: 4-15. doi.org/10.2204/iodp.sd.9.01.2010.

Maiorano P. & Monechi S. (1998) - Revised correlations of Early and Middle Miocene calcareous nannofossil events and magnetostratigraphy from DSDP site 563 (North Atlantic Ocean). *Marine Micropaleontology*, 35(3-4): 235-255.

Martini E. (1971) - Standard Tertiary and Quaternary calcareous nannoplankton zonation. *Proceedings II Planktonic Conference, Roma*: 739-785.

Mascle J., Lohmann G.P., Clift P.D. & Shipboard Scientific Party (1996) - Site 959. In: Mascle J., Lohmann G. P., Clift P. D. et al. (Eds) -*Ocean Drilling Program Initial Reports*, 159: 65-150. College Station, TX (Ocean Drilling Program).

Matsuoka H. & Okada H. (1990) - Time-progressive morphometrical changes of the genus *Gephyrocapsa* in the Quaternary sequence of the tropical Indian Ocean, Site 709. In: Duncan R.A., Backman J., Peterson L.C et al. (Eds) - *Ocean Drilling Program Scientific Results*, 115: 55-270. College Station, TX (Ocean Drilling Program).

Okada H. & Bukry D. (1980) - Supplementary modification and introduction of code numbers to the low latitude coccolith biostratigraphy zonation (Bukry 1973, 1975). *Marine Micropaleontology*, 51: 321-325.

Olafsson G. (1991) - Late Oligocene through Late Miocene Calcareous Nannofossil Biostratigraphy and Biochronology. *Meddelanden från Stockholms Universitets Institution för Geologiog Geokemi*, 283, 157 pp.

Paillard D., Labeyrie L. & Yiou P. (1996) - Macintosh Program performs time-series analysis. *Eos, Transactions American Geophysical Union*, 77(39): 379-379.

Pälike H., Lyle M., Nishi H., Raffi I., Gamage K. & Klaus A. (2010) - Pacific equatorial age transect. *Proceedings of the Integrated Ocean Drilling Program*: 320/321. Integrated Ocean Drilling Program Management International, Tokyo. doi.org/10.2204/iodp.proc.320321.2010.

Raffi I. & Rio D. (1979) - Calcareous nannofossil biostratigraphy of DSDP Site 132-Leg 13 (Tyrrhenian Sea-Western Mediterranean). *Rivista Italiana di Paleontologia e Stratigrafia*, 85: 127-172.

Raffi I., Backman J., Rio D. & Shackleton N.J. (1993) - Plio-Pleistocene nannofossil biostratigraphy and calibration to oxygen isotope stratigraphies from Deep Sea Drilling Project Site 607 and Ocean Drilling Program Site 677. *Paleoceanography*, 8(3): 387-408.

Raffi I. & Flores J.-A. (1995) - Pleistocene through Miocene calcareous nannofossils from eastern equatorial Pacific Ocean. In: Pisias N.G., Mayer L.A., Janecek T.R., Palmer-Julson A. & van Andel T.H. (Eds) - *Ocean Drilling Program Scientific Results,* 138: 233-286. College Station, TX: doi.org/10.2973/odp.proc.sr.138.112.1995.

Raffi I., Rio D., D'Atri A., Fornaciari E. & Rocchetti S. (1995) - Quantitative distribution patterns and biomagnetostratigraphy of middle and late Miocene calcareous nannofossils from Equatorial Indian and Pacific Oceans (Legs 115, 130, and 138). In: Pisias N.G., Mayer L.A., Janecek T.R., Palmer-Julson A. & van Andel T.H. (Eds) - *Proceedings of the Integrated Ocean Drilling Program,* 138: 479-502. College Station, TX (Ocean Drilling Program). doi:10.2973/odp.proc.sr.138.125.1995.

Raffi I., Mozzato C., Fornaciari E., Hilgen F.J. & Rio D. (2003) - Late Miocene calcareous nannofossil biostratigraphy and astrobiochronology for the Mediterranean region. *Micropaleontology*, 49(1): 1-26.

Raffi I., Backman J., Fornaciari E., Pälike H., Rio D., Lourens L. & Hilgen F. (2006) - A review of calcareous nannofossil astrobiochronology encompassing the past 25 million years. *Quaternary Science Reviews*, 25(23-24): 3113-3137. doi: 10.1016/j.quascirev.2006.07.007.

Reghellin D., Dickens G.R., Coxall H.K. & Backman J. (2020) - Understanding bulk sediment stable isotope records in the Eastern Equatorial Pacific, from seven million years ago to present day. *Paleoceanography and Paleoclimatology*, 35(2): 1-22. doi.org/10.1029/2019PA003586.

Reghellin D., Coxall H. K., Dickens G. R. & Galeotti S. & Backman J. (2022) - The Late Miocene-Early Pliocene Biogenic Bloom in the Eastern Equatorial Pacific: New Insights from Integrated Ocean Drilling Program Site U1335. *Paleoceanography and Paleoclimatology*, 37(3): 1-16. doi.org/10.1029/2021PA004313.

Rio D. (1982) - The fossil distribution of coccolithophore genus *Gephyrocapsa* Kamptner and related Plio-Pleistocene chronostratigraphic problems. In: Prell Warren L., Gardner James V., Adelseck Charles G. et al. (Eds) - *Initial Reports of the Deep Sea Drilling Project*, 68: 325-343. Washington, DC (US Government Printing Office). doi: 10.2973/dsdp.proc.68.109.1982.

Rio D., Fornaciari E. & Raffi I. (1990a) - Late Oligocene through early Pleistocene calcareous nannofossils from western equatorial Indian Ocean (Leg 115). In: Duncan R.A., Backman J., Peterson L.C. et al. (Eds) - *Proceedings of the Integrated Ocean Drilling Program Results,* 115: 175–235. College Station, TX (Ocean Drilling Program). doi:10.2973/odp.proc.sr.115.152.1990.

Rio D., Raffi I. & Villa G. (1990b) - Pliocene-Pleistocene calcareous nannofossil distribution patterns in the western Mediterranean. In: Kastens K.A., Mascle J. et al. (Eds) - *Proceedings of the Integrated Ocean Drilling Program*, 107: 513-533. College Station, TX (Ocean Drilling Program). doi:10.2973/odp.proc.sr.107.164.1990.

Sosdian S.M., Babila T.L., Greenop R., Foster G.L. & Lear C.H. (2020) - Ocean carbon storage across the middle Miocene: a new interpretation for the Monterey Event. *Nature Communication*, 11: 134.

Steinthorsdottir M., Coxall H.K., de Boer A.M., Huber M., Barbolini N., Bradshaw C.D., Burls N.J., Feakins S.J., Gasson E., Henderiks J., Holbourn A.E., Kiel S., Kohn M.J., Knorr G., Kürschner W.M., Lear C.H., Liebrand D., Lunt D.J., Mörs T., Pearson P.N., Pound M.J., Stoll H. & Strömberg C.A.E. (2021) - The Miocene: The Future of the Past. *Paleoceanography and Paleoclimatology*, 36(4): 1-71.

Suchéras-Marx B., Viseur S., Walker C. E., Beaufort L., Probert I. & Bolton C. (2022) - Coccolith size rules – What controls the size of coccolithsduring coccolithogenesis? *Marine Micropaleontology*, 170: 102080. https://doi.org/10.1016/j.marmicro.2021.102080.

Takayama T. (1993) - Notes on Neogene calcareous nannofossil biostratigraphy of the Ontong Java Plateau and size variations of *Reticulofenestra* coccoliths. In: Berger W.H., Kroenke L.W., Mayer L.A. et al. (Eds) - *Proceedings of the Integrated Ocean Drilling Program Results*, 130: 179-229. College Station, TX (Ocean Drilling Program). https://doi.org/10.2973/odp.proc.sr.130.020.1993.

Tian J., Ma X., Zhoua J., Jiang X., Lyle M., Shackford J. & Wilkens R. (2018) - Paleoceanography of the east equatorial Pacific over the past 16 Myr and Pacific-Atlantic comparison: High resolution benthic foraminiferal O C records at IODP Site U1337. *Earth and Planetary Science Letters*, 499: 185-196. doi: 10.1016/j.epsl.2018.07.025.

Villa G., Fioroni C., Pea L., Bohaty S. M. & Persico D. (2008) - Middle Eocene-late Oligocene climate variability: Calcareous nannofossil response at Kerguelen Plateau, Site 748. *Marine Micropaleontology*, 69: 173-192. http://doi.org/10.1016/j.marmicro.2008.07.00.

Vincent E. & Berger W.H. (1985) - Carbon dioxide and polar cooling in the Miocene: the Monterey hypothesis. *The Carbon Cycle and Atmospheric CO_2*, 32: 455-468.

Wagner T. (2002) - Late Cretaceous to early Quaternary organic sedimentation in the eastern Equatorial Atlantic. *Palaeogeography, Palaeoclimatology, Palaeoecology*, 179: 113-147.

Westerhold T., Marwan N., Drury A.J., Liebrand D., Agnini C., Anagnostou E., Barnet J.S.K., Bohaty S.M., De Vleeschouwer D., Florindo F., Frederichs T., Hodell D.A., Holbourn A.E., Kroon D., Lauretano V., Littler K., Lourens L.J., Lyle M., Pälike H., Röhl U., Tian J., Wilkens R.H., Wilson P.A. & Zachos J.C. (2020) - An astronomically dated record of Earth's climate and its predictability over the last 66 million years. *Science*, 369(6509): 1383-1388. https://doi.org/10.1126/science.aba6853.

Wilkens R.H., Dickens G.R. Tian J. & Backman J. (2013) - Data report: revised composite depth scales for Sites U1336, U1337, and U1338. In: Pälike H., Lyle M., Nishi H., Raffi I., Gamage K., Klaus A. & the Expedition 320/321 Scientists (Eds) - *Proceedings of the Integrated Ocean Drilling Program*, 320/321: 1-158 Tokyo (Integrated Ocean Drilling Program Management International, Inc.).

Young J. (1990) - Size variation of Neogene *Reticulofenestra* coccoliths from Indian Ocean DSDP Cores. *Journal of Micropalaeontology*, 9(1): 71-85.

Young J.R., Bown P.R. & Lees J.A. (2022) - Nannotax3 website. International Nannoplankton Association. Accessed in 2022. URL: www.mikrotax.org/Nannotax3.

Zachos J.C., Kroon D., Blum P. et al. (2004) - *Initial Reports of the Deep Sea Drilling Project*, 208. College Station, TX (Ocean Drilling Program). doi:10.2973/odp.proc.ir.208.2004.